Springer

KSME

Journal of Mechanical Science and Technology 32 (10) (2018) 4883~4892
www.springerlink.com/content/1738-494x(Print)/1976-3824(Online)
DOI 10.1007/s12206-018-0936-8

Cutting mechanism and surface integrity in milling of Ti-5553 processed by selective laser melting †

Thilo Grove[1], Berend Denkena[1], Oliver Maiß[1], Alexander Krödel[1,*], Holger Schwab[2] and Uta Kühn[2]

[1]*Institute of Production Engineering and Machine Tools (IFW), Leibniz Universität Hannover, An der Universität 2, 30823 Garbsen, Germany*
[2]*IFW Dresden, Institute for Complex Materials, D-01069 Dresden, Germany*

(Manuscript Received February 12, 2018; Revised May 21, 2018; Accepted June 30, 2018)

Abstract

Titanium alloys are of significant importance in several high performance applications such as aerospace components or medical implants. Advances in additive technologies lead to an increase of additively built workpieces, offering new possibilities regarding functional integration and lightweight structures. Several authors have shown that microstructural, mechanical and thermal material properties differ significantly from those of cast alloys. Although additively produced parts are near net-shape, most of them are machined after the building process, to achieve the requirements regarding surface finish and dimensional accuracy. Titanium is generally known as a hard-to-cut material due to its thermo-mechanical properties. Although there is a profound knowledge about the machinability of conventionally cast and wrought titanium alloys, there is a lack of understanding regarding the machining of additively built titanium. In this paper, the machinability of an additively built Ti-5Al-5V-5Mo-3Cr alloy (Ti-5553) is analyzed regarding chip formation, cutting forces and tool wear. Three different generation methods, conventional wrought, selective laser melting and selective laser melting with in-process (in-situ) heat treatment are investigated. It is shown that the machinability differs significantly compared to a conventional wrought alloy, which is linked to decreased contact length on the tool rake face and higher mechanical tool load (up to + 23 % force increase). Highest tool load is found for titanium alloy, which is built using selective laser melting and in-process heat treatment. Furthermore, the surface integrity after machining is analyzed regarding hardness, roughness and residual stresses. Hereby, high compressive residual stresses for additively built titanium with in-process heat treatment are obtained due to the higher mechanical tool load. Therefore, it could be shown that the generation method (e.g. selective laser melting) needs to be considered for the later process design in finish machining.

Keywords: SLM; Titanium; Machinability; Milling; Residual stress

1. Introduction

Titanium alloys are of significant importance for several high performance applications such as aerospace or medical engineering [1, 2]. A current development in industry is the increased use of additively manufactured titanium parts. Additive manufacturing (AM) offers new possibilities regarding internal structures in titanium parts [2, 3] and can drastically decrease the number of process steps within a production chain [3]. Regarding additive manufacturing of titanium, the technologies selective laser melting (SLM) and electron beam melting (EBM) are most widely used. Because of the process specific surface properties and the necessity of support structures, most of the additively built parts need to be finished after the building process [4]. In a majority of applications, machining technologies such as milling or drilling are used to meet the requirements regarding the surface finish and dimensional accuracy [5]. Several investigations have proven that the resulting material properties of additively manufactured titanium differ significantly from those of conventional cast or wrought materials. Furthermore, the built materials are typically heat treated after AM, leading to further differences in mechanical and microstructural properties [6]. Although the resulting material properties in AM are widely investigated, there is a lack of knowledge about the machinability of those materials. First research results show substantial differences in the machinability of conventional wrought alloys and additively built material [7-11].

Selective laser melting as well as electron beam melting are both layer-by-layer technologies. The SLM-processes in general and especially for titanium are characterized by very high solidification rates (10^3-10^8 K/s) in the melt pool [12] compared to conventional casting (up to 3 K/s) [13, 14]. In dependency of the titanium alloy and the used process parameters in SLM, different microstructures are obtained [15-17]. Regarding Ti-6Al-4V as the most widely used titanium alloy,

*Corresponding author. Tel.: +49 511 762 18337, Fax.: +49 511 762 5115
E-mail address: kroedel@ifw.uni-hannover.de
† Recommended by Associate Editor Yongho Jeon

the rapid solidification leads to an α'-martensitic phase composition of the finished titanium part [6, 18]. It could be shown for near-β-titanium alloys that also a pure β-composition can be stabilized to room temperature applying selective laser melting [17]. In general, the microstructure is characterized by a high anisotropy and long elongated grains in building direction. Grain growth is significantly influenced by the utilized process parameters. The observed mechanism can be controlled by changing building direction of the parts or the hatch style defining the scan tracks within the laser processed area [15].

To achieve the requirements of the aerospace industry regarding ductility and relative density most Ti-6Al-4V parts are heat treated or even hot isostatically pressed (HIP) after the AM-process [1, 6]. Vrancken et al. prove that the properties after the SLM-process greatly influence the obtained result after heat treatment and therefore need to be taken into consideration regarding the aimed final material properties. The HIP-treatment leads to a decrease in material porosity [6], which can increase part fatigue strength [18]. As an alternative for conventional heat treatments and HIP processes, Löber presents a method for an in-process heat treatment in SLM-machines [19], which was later also applied to the titanium alloy Ti-5553 (Ti-5Al-5Mo-5V-3Cr) [20]. It could be shown that the mechanical properties of titanium aluminides could be increased using this technology. Furthermore, crack formation in the building process was decreased due to reduced thermal stresses [19].

The machinability of conventionally produced titanium alloys is widely investigated [21-25]. Machining of titanium is characterized by high thermomechanical loads of the tool due to relatively low temperature softening effect [24] and low thermal conductivity compared to other working materials. Furthermore, chip formation is dominated by segmented chips with short contact length on the rake face in a wide range of cutting speeds [21, 22, 25], leading to high alteration of mechanical loads. In the recent past, some authors include additively built titanium in their investigations [7-11]. Milton et al. analyzed the influence of finish machining on the surface integrity of Ti6-Al-4V in dependency of the building orientation. They could show differing work hardening behavior for SLM-parts compared to a conventionally cast alloy. Also differing process force values in milling presume an influence on the resulting tool load. Bordin et al. and Sartori et al. analyzed the influence of dry and cryogenic turning on tool wear and surface integrity for titanium parts generated with different AM technologies. Sartori et al. could show a significant increase in the tool crater wear for SLM manufactured titanium, which is related to increased hardness and decreased thermal conductivity compared to conventional material [9]. Oyelola et al. investigated the influence of turning on surface integrity of a direct metal deposited (DMD) titanium alloy [10]. Compressive residual stresses are measured using the $\sin^2\varphi$ method. Chip formation and morphology is analyzed, but not compared to conventional alloys.

It can be summarized that there is a strong indication that differing material properties after SLM lead to differences in the machinability as well as on the resulting surface integrity. The available literature deals with the most widely used alloy Ti-6Al-4V. For high load applications, the use of near-β titanium alloys such as Ti-5553 is of increasing importance in industry [26]. The microstructure containing the β-phase as the matrix and the α-phase as fine precipitations causing a high strength and high cycle fatigue behavior. Due to these properties the alloy is for example used in aerospace components such as the landing gear of the Boeing Dreamliner 787 [26-28]. The authors have shown that it is possible to generate dense Ti-5553 alloy with similar mechanical properties to a conventional wrought alloy using SLM, although microstructural properties differ significantly [17, 19, 20]. To enable industrial use of Ti-5553 processed with SLM, also the influence of the generation method on the subsequent finishing processes are of significant importance to control part quality and surface integrity. To the best of our knowledge, there is no available research about the resulting machinability of SLM-processed Ti-5553 and the influence of machining on surface integrity. Therefore, it is the aim of this paper to investigate the influence of additive processing of Ti-5553 on the machinability and the surface integrity.

2. Experimental procedure

Within the presented research, Ti-5553 specimens are generated using selective laser melting with different process strategies. In particular, the in-situ heat treatment presented in Refs. [19, 20] was used to reduce thermally induced stresses within the building process. Afterwards, milling experiments are conducted and evaluated regarding process forces, tool wear and chip formation in comparison to conventional alloy Ti-5553. Lastly, the influence on the achieved surface integrity is analysed.

2.1 Materials and SLM-process

Within the investigations, specimens of the near-β titanium alloy Ti-5553 are produced using SLM. Starting point for the building process is a gas-atomized powder by applying the EIGA-method. The utilized particle fraction is of 25 µm to 45 µm (spherical shape, d_{50} = 35.71 µm). Detailed information about the pre-alloy, the powder atomization and the chemical composition are presented in Refs. [17, 20]. All investigated samples are processed using a SLM Solution 250^{HL} machine tool. The machine is equipped with a laser power of P = 400 W (theoretical power, cw mode, 1064 nm wavelength). In the focal point, the diameter of the laser beam is about 80 µm. The applied SLM-process parameters are specified in Ref. [17]. To reduce thermal residual stress, the scanning strategy designated as checkerboard is chosen with a field size of (4 x 4) mm² [29]. For each applied powder layer, the scanning vectors are shifted by 90°. Within the investiga-

tions, one set of specimens was generated with and one without in-situ heat treatment as shown in Refs. [19, 20]. To accomplish the in-situ heat treatment of the SLM-process, the substrate plate temperature is hold at 500 °C during the building process. This is established by an additional heating device designed by IFW Dresden. The substrate heating device was switched on in advance to ensure a constant temperature before the start of the processing. Specimens produced by this routine are labelled "SLM HT" as followed. The SLM-specimens processed without the in-situ heat treatment are indicated as "as-SLM". For the comparison of the additive condition with the conventional state, a conventional wrought alloy Ti-5553 is used.

To analyze the microstructure, samples are cut out at specimens' bottom, middle, and top position respective to the building direction. The samples are prepared by grinding and polishing (oxide-polishing-suspension with 10 % H_2O_2). Finally, a treatment with glow discharge optical emission spectroscopy (GD-OES) took place to obtain an appropriate contrast of the microstructure for a detailed investigation [30]. A Zeiss Gemini 1530 (varied in voltage and aperture) is used for detailed microstructure image investigation equipped with a BRUKER AXS XFlash 4010 detector for energy dispersive X-ray spectroscopy (Software BRUKER ESPRIT 2.1).

2.2 Milling experiments

Milling tests were conducted on a 4-axis milling machine tool Heller MC16 (Fig. 1). Coolant (5 % emulsion) was supplied externally. Tungsten carbide solid end mills WALTER MC726 (Substrate WK40TF, Hardness 1810 HV_1, TiAlN coating, Hardness 3400 $HV_{0,05}$) were applied in all experiments. The tool is specially developed for the machining of hard to cut materials such as titanium. Process forces were measured using KISTLER three-component dynamometer 9257B. Tool wear was analyzed using a Keyence VHX-600 microscope with 30x-200x magnification. For investigation of process forces, surface integrity and chip formation, new tools were applied to exclude tool wear effects on the obtained results. Process force measurements were repeated once. Maximum deviation between the two measurements was 5 % of the obtained force value. For the results mean values are considered. Cutting speeds of v_c = 50..100 m/min were chosen to analyze a wide range of cutting conditions in the machining of titanium alloys within industrial standards.

2.3 Surface integrity analysis

To investigate the resulting surface integrity, surface roughness, residual stresses, hardness and microstructure, analyzes are conducted. Surface roughness is measured tactile with a Mahr Perthometer concept according to DIN 4766 and optically with a confocal microscope NanoFocus µSurf. A tactile measurement length of $L = 5.6$ mm is used with a cutoff length $\lambda_c = 0.8$ mm. A Gaussian filter is applied to eliminate

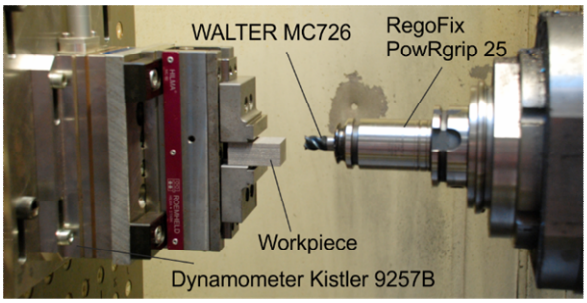

Machine tool and process	Process parameters	Tool
Heller MC16	v_c = 50, 100 m/min	Walter MC726
Down milling	f_z = 0.15 mm	D = 12 mm
With coolant	a_p = 1.5 mm	z = 4
(5% emulsion)	a_e = 0.5 mm	WK40TF

Krö/85182 ©IFW

Fig. 1. Experimental setup milling tests.

the waviness. Each measurement is repeated five times at one specimen to determine the statistic accuracy. The arithmetic roughness Ra and the mean roughness Rz are measured. For the optical measurements an area of 2 mm x 2 mm is investigated and the arithmetic roughness Sa is analyzed. An X-ray diffractometer GE XRD 3000P with CuKα radiation is used to analyze the residual stresses and phase transformations with $\sin^2\varphi$-method. The α-phase reflection 213 with a 2θ-angle of 139.317° is measured for titanium specimens with α and β-phase, whereas the β-phase dominated composition titanium is measured at β-phase reflection 321 with 2θ-angle of 126.0°. To investigate the effects on microstructure, the chips and specimens are etched, polished and analyzed with a Keyence microscope VHX-600 DSO with a 100x - 1000x magnification. Vickers hardness measurements are conducted to generate hardness depth profiles using $HV_{0.025}$.

3. Results and discussion

3.1 Material properties of SLM Ti-5553

The investigated specimens with a size of (20x30x50) mm³ were produced by selective laser melting without (as-SLM) and with substrate heating (SLM + HT) and by casting for the reference material (conventional). The microstructure of the investigated specimens is presented in Figs. 2-4. The conventional alloy is characterized by needle like, fine grain structure and globular segregation of the α-phase (Fig. 2). The as-SLM (Fig. 3(b)) and SLM + HT (Fig. 4) specimens are characterized by long-elongated grains in building direction. Additionally, a cellular to cellular/dendritic solidification is distinctive for the as-SLM processing conditions (Fig 3(b)). The microstructure of the SLM + HT specimen is determined by α-phase precipitations homogenously distributed in the β-phase grains acting as matrix. The precipitations can be distinguished by rectangular arranged plates homogenously distributed in the grains of the β-phase. The length of the plates is up to 3-4 µm, the thickness less than 100 nm. The appearance can be affili-

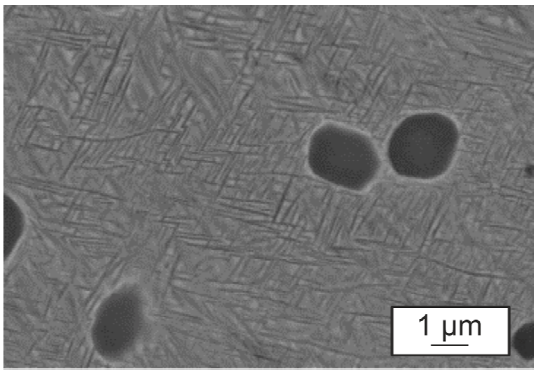

Fig. 2. Microstructure of the wrought Ti-5553 reference alloy with the α-phase as globular particles and platelike precipitations (scanning electron microscopy (SEM)).

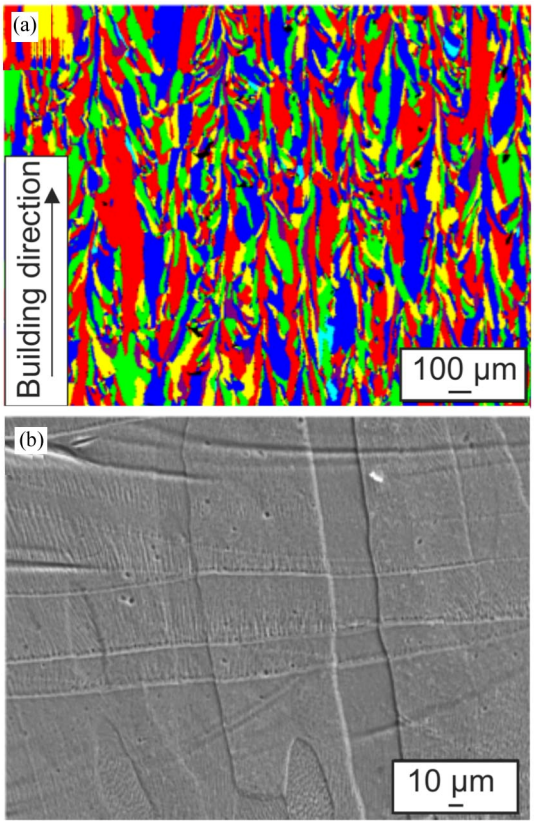

Fig. 3. Characteristic: (a) Grain morphology in false tinting; (b) cellular/cellular-dendritic solidification of the as-SLM specimen (images made by scanning electron microscopy (SEM, 3B) and electron backscatter diffraction (EBSD, 3A)).

ated to the high substrate temperature and thereby occurring ageing processes [27].

Fig. 5 presents the XRD pattern for differently generated Ti-5553 samples. The conventionally wrought alloy Ti5553 and the heat treated alloy SLM + HT show β- and α-phase reflections ($P6_3/mmc$), whereas the Ti-5553 as-SLM is dominated by the β-phase (Im-3m). Additionally, it exhibits weak reflections of the hexagonal ω-phase (P6/mmm). In the alloy Ti-5553, the ω-phase can arise during rapid cooling (athermal)

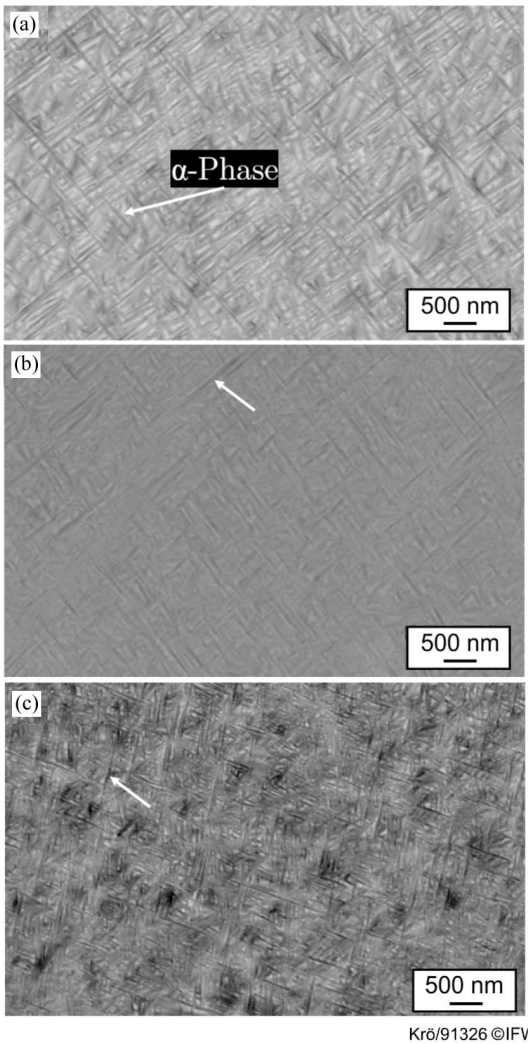

Fig. 4. Typical microstructure of the SLM + HT sample along the building direction at (a) 5 mm; (b) 1.5 mm; (c) 2.5 mm height from the building plate, showing the α-phase precipitations (white arrows) (SEM).

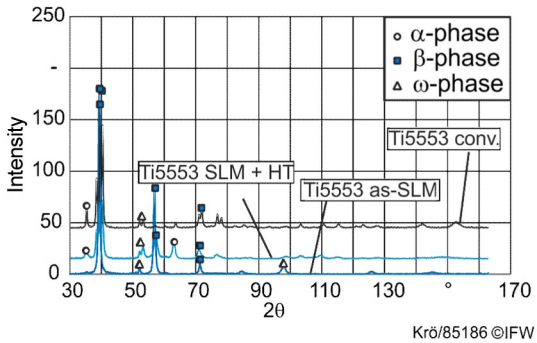

Fig. 5. XRD pattern of differently generated Ti-5553 specimens (conventionally wrought, as-SLM and SLM+HT).

or during isothermal holding (isothermal) below the α-phase ageing temperature in the α/β-phase region [31-33]. Nevertheless, an exact determination is only possible by using TEM.

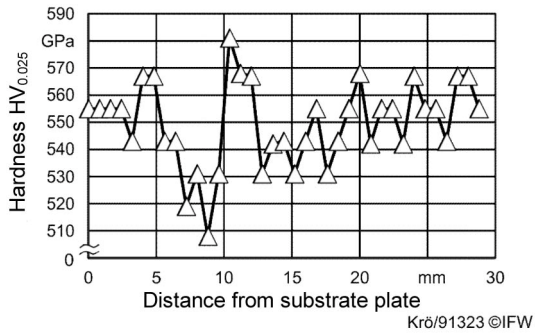

Fig. 6. Hardness in building direction for SLM+HT specimen.

The hardness of the specimens was measured as 325 $HV_{0.025}$ for as-SLM, 604 $HV_{0.025}$ for SLM+HT and 441 $HV_{0.025}$ for the conventional wrought alloy (mean value of ten measurements in the center of each specimen) at the specimen's surface. Since the value of the hardness of the as-SLM specimen is close to the value of a pure β-phase microstructure fabricated by SLM in previous investigations (290 $HV_{0.2}$), it can be pointed out that there is no influence of the ω-phase [20]. In general, Williams et al. documented that at least 25-30 Vol.-% of ω-phase is necessary to influence the mechanical properties [34]. Furthermore, for the SLM+HT specimen a hardness profile in building direction was measured in the center of the specimen. As it can be seen in Fig. 6, there is a relatively high variation in the hardness values between 510 and 580 $HV_{0.025}$. However, there is no tendency for a systematic variation of the specimens' hardness in building direction for example due to unstable temperature distribution during the generation process. The hardness is lower compared to the surface hardness, which might be caused by a slower cooling rate and a resulting tempering process.

3.2 Machinability of SLM Ti-5553

Within the applied investigations, milling tests as depicted in chapter 2 were conducted with different cutting speeds. To analyze potential differences in chip formation due to differing thermomechanical properties of the specimens chips were collected after machining as presented in Fig. 7. It can be seen that the resulting chip curl radius when machining the as-SLM specimen is significantly higher compared to the other specimens. The smallest chip curl radius with slight differences to wrought material is detected for machining of SLM + HT. Chip curl radius in machining is strongly influenced by the thermal properties of the workpiece material and also the frictional behavior between the tool rake face and the chip [35]. A first indication could be a difference in thermal conductivity of SLM material, which was shown for Ti-6Al-4V in Refs. [8, 9] due to martensitic microstructures. Generally, a bigger chip curl radius results in an increase of the chip contact length on the rake face, which influences the stress distribution. Therefore, the highest stress concentration is to be expected for SLM+HT due to the shortest contact length between chip and rake. Best machinability due to lowest mechanical stresses is

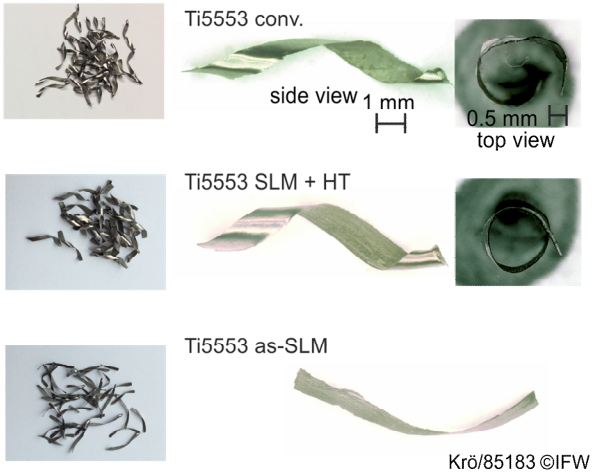

Fig. 7. Chip morphology and chip curl of the investigated processing conditions (conventional heat treated, as-SLM and SLM + HT) (v_c = 100 m/min).

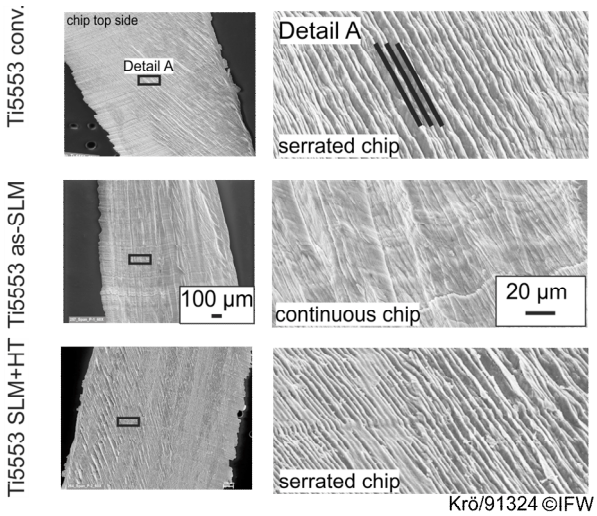

Fig. 8. Chip formation of the investigated processing conditions (conventional wrought, as-SLM and SLM+HT) (v_c = 100 m/min) and analysis of chip serration.

expected for the as-SLM specimen with highest chip curl radius.

Furthermore, chip morphology was analyzed in detail using SEM imagery (Fig. 8). Ti-5553 conventional and Ti-5553 SLM+HT show serrated chip formation, whereas Ti-5553 as-SLM exhibits almost continuous chip formation.

Besides the analysis of the chips, process force measurements were conducted in feed, feed normal and passive force direction for the cutting speeds v_c = 50 and 100 m/min as presented in Fig. 9. Highest process forces are detected for the heat treated alloy with a mean increase compared to the conventional alloy of 23 % for v_c = 50 m/min and 16 % for v_c = 100 m/min, respectively. The as-SLM specimen exhibits lower process forces compared to the conventional wrought alloy of -6 % in average for v_c = 50 m/min and v_c = 100

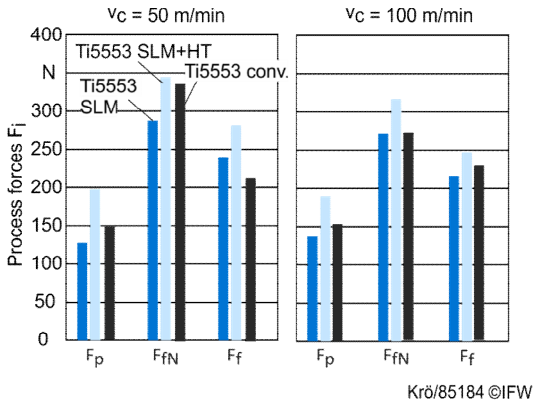

Fig. 9. Mean process forces for milling of differently generated Ti-5553 specimens for v_c = 50 m/min and v_c = 100 m/min.

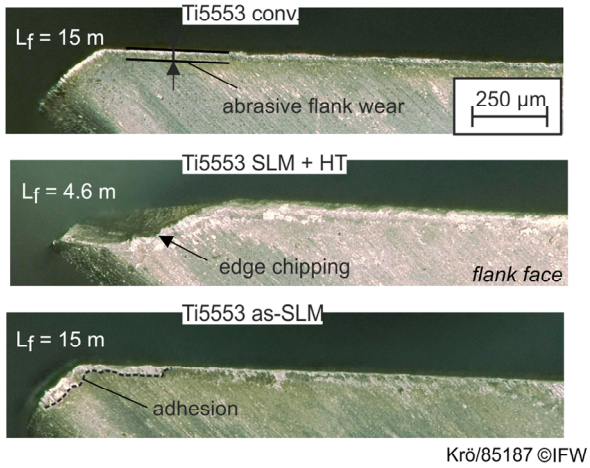

Fig. 10. Obtained wear forms and mechanism in milling experiments for different titanium specimens, v_c = 100 m/min.

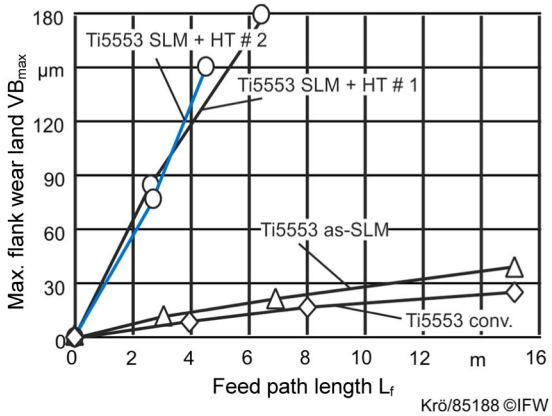

Fig. 11. Flank wear for different titanium specimens.

m/min. In so far, generally better machinability of the as-SLM condition is to be expected against the conventional wrought titanium because of lower resulting mechanical load and increased contact length of the chip leading to decreasing stress load on the tool rake face. Also, chip formation is characterized by a more continuous chip, leading to decreased dynamic stress spectra. Furthermore, the load resulting from machining the SLM + HT sample is to be expected more demanding for the tool because chip curl radius is comparable to conventional alloy (equal chip contact length) but mechanical loads are significantly higher. Regarding temperature softening effect, all alloys exhibit a small process force decrease with raising cutting speed, which is in contrast to similar investigations of Gey for the Ti-6Al-4V alloy [24, 36] in the observed cutting speed range. The mean decrease in cutting force is 5 % for the conventional alloy and 4 % (as-SLM), 7 % (SLM+HT) respectively. In so far, differences in thermal softening are of minor importance regarding conventional and SLM alloys, whereas the generation method needs to be taken into account concerning force values and mechanical tool load.

Furthermore, the tools were applied in milling wear tests with the cutting speed v_c = 100 m/min (and the process data as depicted in Fig. 1). Results of the wear tests are presented regarding obtained wear mechanism via digital microscope (Fig. 10) and tool wear diagrams for the flank wear land (Fig. 11).

Tool wear for the machining of the conventional titanium alloy is dominated by slight abrasive flank wear over the observed feed path L_f = 15 m. The as-SLM specimen leads to a slight increase in flank wear land on the tool compared to the conventional alloy. Most significant differences are observed concerning the machining of the SLM+HT specimen. Tool wear is dominated by severe chipping at the corner radius after a short feed path of L_f = 4.6 m. Also, the flank wear beside the chipping failure is significantly higher compared to the machining of the other specimen. For exclusion of possible pre-existing damages of the milling tool, the test was repeated once with a new tool. As shown in Fig. 11, an identical wear progression was observed in the second machining test for SLM+HT. It can be concluded that tool wear is significantly influenced by the generation method of additively manufactured titanium alloy Ti-5553. Especially the machinability of the heat treated SLM+HT state is worse compared to conventional wrought material and as-SLM specimen without heat treatment. As a possible reason for the tool wear effect the increased cutting forces (compare Fig. 9) in combination with the lowest contact length resulting from chip curl radius (compare Fig. 7) for SLM+HT are expected. Furthermore, the hardness of the SLM+HT specimen is significantly higher compared to the other specimens, which is also a reason for higher mechanical load and abrasive wear.

3.3 Machining impact on surface integrity of SLM Titanium

The effect of finish machining on surface roughness for the analyzed specimens is presented in Fig. 12. Mean roughness Rz and arithmetic roughness Ra or Sa are comparable for each material for 50 m/min and 100 m/min, respectively. However, the measured roughness values differ between the generation methods. For the reference material the surface roughness is

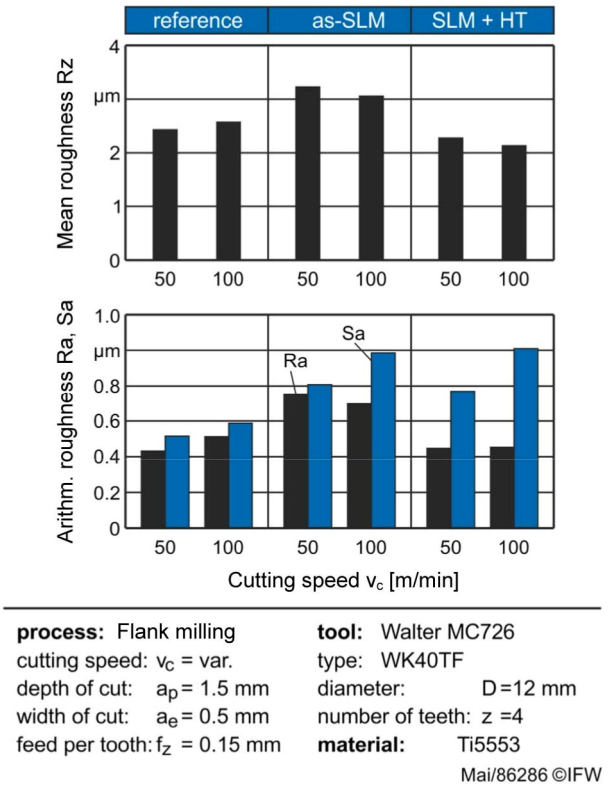

Fig. 12. Surface roughness in milling for reference, as-SLM and SLM+HT specimens.

smaller than for the SLM-processed specimens. Focusing on the tactile roughness values Rz and Ra of the SLM+HT sample enables lower surface roughness values than the reference- and the as-SLM-material. The optical measurement for the SLM+HT condition shows small peaks on the surface creating a poor surface finish. Summarizing the obtained results, the machinability of additively built parts in terms of roughness is worse compared to the conventional alloy.

Surface residual stress measurements are conducted parallel and perpendicular to the feed direction for the reference and both SLM-states before and after milling at the position of the milled surface. The results are demonstrated in Fig. 13. In the unmachined state, all specimens exhibit an equal residual stress level with only slight tendencies regarding compression or tension. As shown in the picture, the machining of the conventional alloy at v_c = 50 m/min leads to minor changes in the stress state and a small increase of compressive stresses parallel to feed direction. Increasing the cutting speed results in increasing compressive residual stresses in both directions.

For the as-SLM material, a differing behavior parallel and perpendicular to the feed motion is observed. The perpendicular direction shows increase in tensile stress state, whereas the parallel direction is shifted to compressive stresses. Both effects increase with increasing cutting speed. The directional behavior of the material is subjected to the anisotropy of the material ranging from the building direction and the resulting elongation of grains. In this case, the perpendicular direction

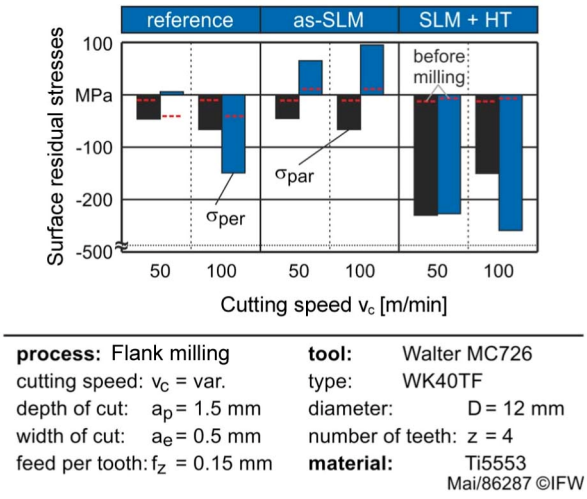

Fig. 13. Surface residual stresses after milling.

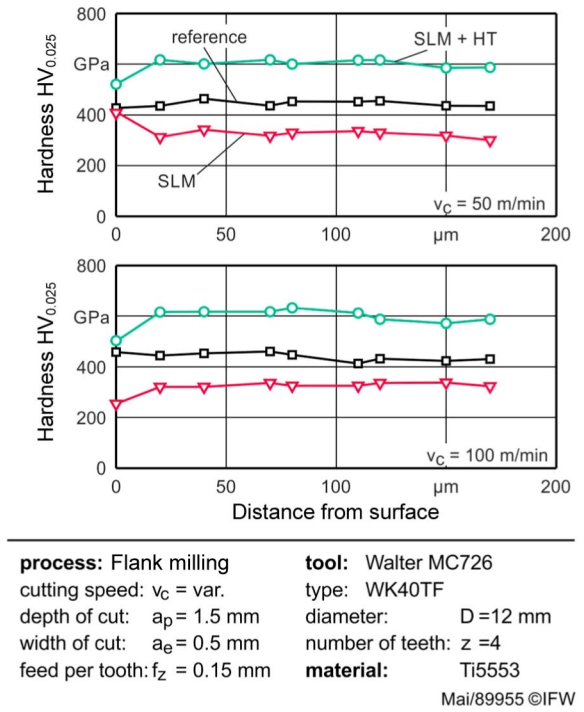

Fig. 14. Hardness depth profiles for the analyzed titanium specimens.

of milling is parallel to the building direction.

The in-situ heat treated alloy exhibits differing behavior with strong compressive stresses after the machining with both cutting speeds. A directional difference in parallel or perpendicular direction is not obtained.

Summarizing the results, it can be stated that the generation method influences the surface quality as well as the induction of residual stresses in the material. Directional behavior can be seen for as-SLM material, whereas the in-situ heat treatment results in compressive stresses in both directions (parallel and perpendicular to building direction).

Furthermore, the hardness depth profile of the milled sur-

face was analyzed for all specimens (Fig. 14). The hardness is significantly influenced by the process chain before the milling process. For all three tested material conditions the hardness is constant for distances from the surface z from 20 - 170 µm. Within this depth, the milling process has no influence on the resulting hardness depth profiles. Regarding the surface hardness, the reference material has only slight differences to the core hardness. For both SLM alloys different tendencies for the surface roughness are observed. The SLM+HT alloy exhibits a significant softening of the surface for both cutting speeds. In contrast, the as-SLM alloy shows hardening behavior of the surface at low cutting speed and softening for high cutting speed.

4. Conclusions

Based on the investigations, the following conclusions can be drawn:

- Machinability of Ti-5553 produced by SLM differs significantly from conventional alloys. The differences were connected to a change in the chip formation process, leading to differing thermo-mechanical load of the cutting edge.
- The in-situ heat treatment of Ti-5553 leads to significant increases in hardness (+37 %) and cutting forces (+23 %) resulting in higher tool wear.
- The mechanical load of the cutting edge is increased for the SLM+HT specimen because of reduced contact length on the tool rake. The mechanical load leads to severe cutting edge chipping in wear experiments.
- Tool wear in machining as-SLM and conventional Ti-5553 could not be proven to differ within the applied investigations.
- Residual stresses for as-SLM material show directional behavior, which indicates a dependency on the building direction. The higher mechanical loads in machining SLM+HT lead to compressive residual stresses of up to -400 MPa after machining.

The obtained results prove that machinability of titanium alloys can be drastically influenced by the generation method, e.g. selective laser melting. Concerning future research, an interesting field could be the adjustment of SLM and heat treatment parameters in order to achieve best machinability in the finishing of the part. Furthermore, the influence of different machining processes such as drilling and turning needs to be investigated. For industrial use, especially the knowledge of differing residual stresses is of importance, because of possible distortion in typically very thin-walled SLM-parts. Moreover, the machining parameters need to be reduced for machining SLM+HT specimen to avoid extensive tool wear.

Acknowledgments

The author thank WALTER AG for providing the applied milling tools for the experiments.

Nomenclature

v_c	: Cutting speed
f_z	: Feed per tooth
a_e	: Radial depth of cut
a_p	: Axial depth of cut
D	: Tool diameter
z	: Number of teeth
L_f	: Feed path length
F_p	: Passive force
F_{fN}	: Feed normal force
F_f	: Feed force

References

[1] E. Uhlmann, R. Kersting, T. B. Klein, M. F. Cruz and A. V. Borile, Additive manufacturing of titanium alloy for aircraft components, *Procedia CIRP*, *15th Machining Innovations Conference for Aerospace Industry*, Hanover, Germany (2015) 55-60.

[2] B. H. Jared, M. A. Aguilo, L. L. Beghini, B. L. Boyce, B. W. Clark, A. Cook, B. J. Kaehr and J. Robbins, Additive manufacturing: Toward holistic design, *Sripta Materialia*, 135 (2017) 141-147.

[3] M. K. Thompson, G. Moroni, T. Vaneker, G. Fadel, R. I. Campbell, I. Gibson, A. Bernard, J. Schulz, P. Graf, B. Ahuja and F. Martina, Design for additive manufacturing: Trends, opportunities, considerations, and constraints, *CIRP Annals - Manufacturing Technology*, 65 (2) (2016) 737-760.

[4] D. Herzog, V. Seyda, E. Wycisk and C. Emmelmann, Additive manufacturing of metals, *Acta Materialia*, 117 (2016) 371-392.

[5] Inside Metal Additive Manufacturing, Mechanical finishing of additively manufactured metal parts, *http://www.insidemetaladditivemanufacturing.com/blog/mechanical-finishing-of-additively-manufactured-metal-parts* (2016).

[6] B. Vrancken, L. Thijs, J. P. Kruth and J. Van Humbeeck, Heat treatment of Ti6Al4V produced by selective laser melting: Microstructure and mechanical properties, *Journal of Alloys and Compounds*, 54 (2012) 177-185.

[7] A. Polishetty, M. Shunmugavel, M. Goldberg, G. Littlefair and R. K. Singh, Cutting force and surface finish analysis of machining additive manufactured titanium alloy Ti-6Al-4V, *Procedia Manufacturing*, *International Conference on Sustainable Materials Processing and Manufacturing*, *SMPM 2017*, South Africa, Kruger National Park (2017) 284-289.

[8] A. Bordin, S. Bruschi, A. Ghiotti and P. F. Bariani, Anlysis of tool wear in cryogenic machining of additive manufactured Ti6Al4V Alloy, *Wear*, 328-329 (2015) 89-99.

[9] S. Sartori, A. Bordin, L. Moro, A. Ghiotti and S. Bruschi, The influence of material properties on the tool crater wear when machining Ti6Al4V produced by Additive manufacturing technologies, *Procedia CIRP*, *7th HPC 2016 - CIRP*

Conference on High Performance Cutting, Chemnitz, Germany (2016) 587-590.

[10] O. Oyelola, P. Crawforth, R. M'Saoubi and A. T. Clare, Machining of additively manufactured parts: Implications for surface integrity, *Procedia CIRP*, *3rd CIRP Conference on Surface Integrity*, Charlotte, USA (2016) 119-122.

[11] S. Milton, A. Morandeau, F. Chalon and R. Leroy, Influence of finish machining on the surface integrity of Ti6Al4V produced by selective laser melting, *Procedia CIRP*, *3rd CIRP Conference on Surface Integrity*, Charlotte, USA (2016) 127-130.

[12] D. Gu, *Laser additive manufacturing of high-performance materials*, First Ed., Springer Publishing Company, Berlin, Germany (2015).

[13] S. L. Semiatin, S. L. Knisley, P. N. Fagin, D. R. Barker and F. Zhang, Microstructural evolution during alpha-beta heat treatment of Ti-6Al-4V, *Metallurgical and Materials Transactions A,* 34 (10) (2003) 2377-2386.

[14] S. Zhu, H. Yang, L. G. Guo and X. G. Fan, Effect of cooling rate on microstructure evolution during α/β heat treatment of TA15 titanium alloy, *Journal of Materials Characterization*, 70 (2012) 101-110.

[15] L. Thijs, F. Verhaeghe, T. Craeghs, J. Van Humbeeck and J. P. Kruth, A study of the microstructural evolution during selective laser melting of Ti-6Al-4V, *Acta Materialia*, 58 (9) (2010) 3303-3312.

[16] H. Attar, M. Calin, L. C. Zhang, S. Scudino and J. Eckert, Manufacture by selective laser melting and mechanical behavior of commercially pure titanium, *Journal of Material Science & Engineering A*, 593 (2014) 170-177.

[17] H. Schwab, F. Palm, U. Kühn and J. Eckert, Microstructure and mechanical properties of the near-beta titanium alloy Ti-5553 processed by selective laser melting, *Materials & Design*, 105 (2016) 75-80.

[18] G. Kasperovich, H. Gherekhloo, J. Gussone, J. Hausmann and Y. C. Hagedorn, Selektives Laserschmelzen von konventionellen und intermetallischen Titanlegierungen - Eigenschaften und Optimierung, *Internal Colloquium DLR*, Available on http://www.dlr.de.

[19] L. Löber, Selektives Laserstrahlschmelzen von Titanaluminiden und Stahl, *Dr.-Ing. Dissertation*, TU Dresden, Germany (2015).

[20] H. Schwab, M. Bönisch, L. Giebeler, T. Gustmann, J. Eckert and U. Kühn, Processing of Ti-5553 with improved mechanical properties via an in-situ heat treatment combining selective laser melting and substrate plate, *Materials & Design*, 130 (2017) 83-89.

[21] P.-J. Arrazola, A. Garay, L.-M. Iriarte, M. Armendia, S. Marya and F. Le Maitre, Machinability of titanium alloys (Ti6Al4V and Ti555.3), *Journal of Materials Processing Technology*, 209 (5) (2009) 2223-2230.

[22] R. Komanduri, Some clarifications on the mechanics of chip formation when machining titanium alloys, *Wear*, 76 (1) (1982) 15-34.

[23] F. Zanger, Segmentspanbildung, werkzeugverschleiss, randschichtzustand und bauteileigenschaften: Numerische analysen zur optimierung des zerspanungsprozesses am beispiel von Ti-6Al-4V, *Dr.-Ing. Dissertation*, KIT Karlsruhe, Germany (2012).

[24] E. Abele and B. Fröhlich, High speed milling of titanium alloys, *Advances in Production Engineering & Management*, 3 (2008) 131-140.

[25] S. A. Iqbal, P. T. Mativenga and M. A. Sheikh, A comparative study of the tool-chip contact length in turning of two engineering alloys for a wide range of cutting speeds, *The international Journal of Advanced Manufacturing Technology*, 42 (2009) 30-40.

[26] S. Veeck, D. Lee, R. Boyer and R. Briggs, The castability of Ti-5553 alloy, *Advanced Materials & Processes*, 162 (10) (2004) 47-49.

[27] J. C. Sabol, T. Pasang, W. Z. Misiolek and J. C. Williams, Localized tensile strain distribution and metallurgy of electron beam welded Ti-5Al-5V-5Mo-3Cr titanium alloys, *Journal of Materials Processing Technology*, 212 (11) (2012) 2380-2385.

[28] H. Matsumoto, M. Kitamura, Y. Li, Y. Koizumi and A. Chiba, Hot forging characteristic of Ti-5Al-5V-5Mo-3Cr alloy with single metastable β microstructure, *Materials Science and Engineering: A*, 611 (2014) 337-344.

[29] C. Y. Yap, C. K. Chua, Z. L. Dong, Z. H. Liu, D. Q. Zhang, L. E. Loh and S. L. Sing, Review of selective laser melting: Materials and applications, *Applied Physics Reviews*, 2 (4) (2015).

[30] V. Brackmann, V. Hoffmann, A. Kauffmann, A. Helth, J. Thomas, H. Wendrock, J. Freudenberger, T. Gemming and J. Eckert, Glow discharge plasma as a surface preparation tool for microstructure investigations, *Materials Characterization*, 91 (2014) 76-88.

[31] N. G. Jones, R. J. Dashwood, M. Jackson and D. Dye, β-Phase decomposition in Ti-5Al-5Mo-5V-3Cr, *Acta Materialia*, 57 (13) (2009) 3830-3839.

[32] R. Panza-Giosa, *The effect of heat treatment on the microstructure evolution and mechanical properties of Ti5Al5V-5Mo3Cr, and its potential applications in landing gears*, McMaster University (2009).

[33] G. Lütjering and J. C. Williams, *Titanium*, Second Ed., Springer Berlin Heidelberg, Berlin, Heidelberg (2007).

[34] J. C. Williams, B. S. Hickman and H. L. Marcus, The effect of ω-phase on the mechanical properties of titanium alloys, *Metallurgical Transactions*, 2 (7) (1971) 1913-1919.

[35] P. J. Arrazola, T. Özel, D. Umbrello, M. Davies and I. S. Jawahir, Recent advances in modelling of metal machining processes, *CIRP Annals - Manufacturing Technology*, 62 (2) (2013) 695-718.

[36] C. Gey, Prozessauslegung für das Flankenfräsen von Titan, *Dr.-Ing. Dissertation*, University Hanover (2002).

Berend Denkena is the Director of the Institute of Production Engineering and Machine Tools (IFW).

Alexander Krödel is team leader in the Department "Cutting processes" at the IFW.